Assessing Two Methods for Estimating Bulk Density of Particles in Suspension

by

Alexander Hurley

Submitted in partial fulfilment of the requirements for the
degree of Combined Honours Bachelor of Science in Earth Sciences and Oceanography

at

Dalhousie University
Halifax, Nova Scotia
April, 2012

Distribution License

DalSpace requires agreement to this non-exclusive distribution license before your item can appear on DalSpace.

NON-EXCLUSIVE DISTRIBUTION LICENSE

You (the author(s) or copyright owner) grant to Dalhousie University the non-exclusive right to reproduce and distribute your submission worldwide in any medium.

You agree that Dalhousie University may, without changing the content, reformat the submission for the purpose of preservation.

You also agree that Dalhousie University may keep more than one copy of this submission for purposes of security, back-up and preservation.

You agree that the submission is your original work, and that you have the right to grant the rights contained in this license. You also agree that your submission does not, to the best of your knowledge, infringe upon anyone's copyright.

If the submission contains material for which you do not hold copyright, you agree that you have obtained the unrestricted permission of the copyright owner to grant Dalhousie University the rights required by this license, and that such third-party owned material is clearly identified and acknowledged within the text or content of the submission.

If the submission is based upon work that has been sponsored or supported by an agency or organization other than Dalhousie University, you assert that you have fulfilled any right of review or other obligations required by such contract or agreement.

Dalhousie University will clearly identify your name(s) as the author(s) or owner(s) of the submission, and will not make any alteration to the content of the files that you have submitted.

If you have questions regarding this license please contact the repository manager at dalspace@dal.ca.

Grant the distribution license by signing and dating below.

_____ _____

Name of signatory Date

Table of Contents

Table of Figures

Table of Notation

Beam Attenuation: Cp (m^{-1})

Beam Attenuation to SPM conversion: Cp:SPM ratio ($m^2\ g^{-1}$)

Density of water: ρ_{water} (kg m^{-3})

Digital Floc Camera: DFC

Digital Video Camera: DVC

Gravity: g (m s^{-2})

LD method: LISST-DFC method for calculating bulk density

Martha's Vineyard Coastal Observatory: MVCO

Mean Bulk Density: Density using LD method (kg m^{-3})

Modified in Situ Size Settling Column Tripod: MINSSECT

Particle Bulk Density: ρ_s (kg m^{-3})

Particle Diameter or Size: D (μm and m)

Sequoia Scientific LISST 100x Type B laser particle sizer: LISST

Settling Velocity: Ws (mm s^{-1} and m s^{-1})

Shear Velocity: Shear Velocity (cm s^{-1})

Suspended Particulate Mass: SPM (g m^{-3})

Total Merged Volume: Volume from the LISST and DFC (m3 m^{-3})

Viscosity: μ (kg ($m \cdot s$)$^{-1}$)

Volume Concentration: VC (ppm)

Water Transfer System (McLane Research Laboratories, Inc. Phytoplankton Sampler): WTS

Abstract

Particle density is fundamental for determining clearance rate of a suspension because it affects settling velocity. In most aquatic environments, however, suspended sediment is composed of loosely packed particle aggregates that cannot be sampled without disrupting the particle packing and, as a result, the particle bulk density. The goal of this study is to compare two methods that estimate particle bulk density without directly sampling suspended particles. A new, fast, but untested method (LD method) uses a Sequoia Scientific LISST 100x particle sizer, which records beam attenuation (Cp, m^{-1}) and particle volumes smaller than 250 µm along with a digital floc camera (DFC) used to estimate volume of particles larger than approximately 50µm.. The measured beam attenuation obtained from the LISST is proportional to mass in suspension. Volume in suspension is obtained from the LISST and DFC. Dividing mass in suspension by volume in suspension yields an estimate of the solid mass per unit volume within suspended particles. The water mass per unit volume contained within the flocculated particles can be approximated as being equal water density. Addition of solid and water masses per unit particle volume yields particle bulk density (ρ). A second, more accurate, but more labour-intensive method (DVC method) involves the use of a digital video camera (DVC), which measures particle size and settling velocity. With knowledge of the density and viscosity of the fluid, Stokes Law can be re-arranged to solve for particle density. These instruments were mounted to the Modified in Situ Size Settling Column Tripod (MINSSECT) and deployed in 12 metres of water at the Martha's Vineyard Coastal Observatory during approximately month-long periods in September and October 2007

and 2011. Densities from each method in 2011 are similar, while the LD Method in 2007 yields much higher densities than the DVC method. Higher densities in 2007 result from significantly lower particle volumes from the DFC. Lower DFC volumes in 2007 may reflect actual lower abundances of large particles, or they may arise from poorer image quality caused either by degraded water clarity of different particle composition.

Acknowledgements

The author would like to thank Dr. Paul Hill for the opportunity to work in the Hill lab and with this research. This project was made possible with the help of the following individuals who contributed their time, effort, ideas and equipment: Hill lab (John Newgard and Jessica Carrière-Garwood) and BIO Particle Dynamics Lab (Brent Law, Tim Milligan and Vanessa Page). I also am grateful for the skillful assistance of the captain and crew of the M/V Tioga. The author would also like to thank U.S. Office of Naval Research for providing research funding to Dr. Paul Hill.

Chapter 1 - Introduction

1.1 Introduction

Due to increased wave and current action in the ocean (e.g. storms and tides) sediment is resuspended. The suspended particulate mass (SPM) limits the transmission of light, and water clarity is reduced. This phenomenon is important to scuba divers and to operators of submersible vehicles. For example, if submersible vehicles equipped with optical devices, such as cameras, are deployed when water clarity is poor, little to no information can be collected, which results in wasted money, time and effort. Therefore, the amount of time it takes for particles to settle out of suspension after waves and currents subside is of interest. Particle density is fundamental for determining clearance rate of a suspension. The goal of this thesis is to assess a potential new method for obtaining bulk density of mass in suspension. Accurate application of the new method would improve our ability to gather high resolution time series of this important variable.

1.2 Previous Work

A wide variety of factors affect the resuspension and transportation of sediment. There are four primary mechanisms for introducing particles into suspension: wave resuspension, resuspension by tidal currents, resuspension by lower frequency currents, and river discharge [*Ogston et al.*, 1999]. In nearshore waters away from river mouths, waves and tidal currents are the two dominant mechanisms for resuspending and maintaining particles in suspension. Resuspension due to wave forcing is characterized

by a high correlation between orbital velocity and concentration of the suspended sediment. Transport by tidal currents often requires waves to resuspend the particles, but tidal currents allow the sediment to remain in suspension above the relatively thin wave boundary layer [*Ogston et al.*, 1999]. Because wave and tides are oscillatory, low-frequency/mean current forcing is responsible for the magnitude and direction of net transport. The amount of sediment that is transported by these mechanisms depends on the concentration of particles in suspension as well as the frequency of resuspension events. Often net transport of particles in suspension is greater in low-frequency bands which resuspend a large amount of sediment, compared to lesser values in tidal bands that are more frequent but lower magnitude [*Ogston et al.*, 1999]. Transport of particles in buoyant river plumes is important near rivers.

Give the variety and frequency of sediment transporting mechanisms in the coastal ocean, full understanding of sediment dynamics requires relatively high-resolution, long time series of sediment transport parameters. Particle bulk density, because it affects settling velocity, is a parameter of interest, but the established methods to estimate it are labour-intensive, precluding the acquisition of high-resolution, long time series [*Hill et al.*, 2011]. Recent advancements in understanding of the optical properties of flocculated suspensions, however, suggest that a proxy for density that can be measured at high resolution during extended deployments may be available.

The Sequoia Scientific LISST 100x Type B measures the beam attenuation coefficient (Cp), which can be converted to SPM with an empirical conversion coefficient called the Cp:SPM ratio. Earlier studies (e.g. *Baker and Lavelle, 1984*) theorized that conversion from optical properties to SPM was uncertain based on the theory of solid spheres, due primarily to changing particle size. Uncertainty was compounded after wide ranges for Cp:SPM were obtained in numerous studies. However, recent work has shown that size is not a determining factor in converting optical properties to SPM [*Hill et al.*, 2011]. When plotting Cp versus SPM, a linear correlation is the result, with the slope of the line equal the Cp:SPM ratio. This linear relationship is observed over a wide range of particle sizes. This result is due to the fact that marine particles are often flocculated, meaning many small particles have collided and adhered to form aggregate particles, also known as "flocs". For flocs, Cp is not sensitive to size, so it can be used as a robust proxy for SPM in time-varying suspensions [*Hill et al.*, 2011]. The LISST also measures particle volume, so by dividing estimated SPM by particle volume, an estimate of solid mass per particle volume results. By adding the mass of enclosed water per unit of particle volume, particle bulk density results.

Floc density conventionally is calculated using size and settling velocity data. The settling velocity of a floc depends on its size and density of excess of water. If size, settling velocity and water temperature and salinity are measured, then density can be calculated.

1.3 **Objectives**

This research has three objectives. The first is to gather in situ size-settling velocity data at the same time that particle beam attenuation and suspended particle volume data are collected. The second is to use these data to solve for two estimates of particle bulk density in suspension. The third objective is to examine whether the two estimates of bulk density are similar.

Chapter 2 - Methods

2.1 Site

The area of study as well as methods have been summarized by *Hill et al.* [2011].The area of data collection (Figure 2.1) is located at the Woods Hole Oceanographic Institution's Martha's Vineyard Coastal Observatory (MVCO) 12-m offshore node [*Hill et al.*, 2011]. The MVCO includes various instruments in conjunction with the subsurface node (mounted in 12-m water depth, approximately 1.5 km offshore). A small shore lab is located in Woods Hole that communicates with the subsea and meteorological instruments. Instruments include a 10-m meteorological mast and an air-sea interaction tower (ASIT) at the 15-m isobath [*Hill et al.*, 2011].

2.2 Overview of MINSSECT

The Modified in Situ Size Settling Column Tripod (MINSSECT) is mounted with similar instruments as its predecessor, the In Situ Size and Settling Column Tripod, otherwise known as INSSECT [*Hill et al.*, 2011; *Mikkelsen et al.*, 2004]. The MINSSECT is mounted with a Sequoia Scientific LISST 100x Type B laser particle sizer, a Digital Floc Camera (DFC), a Water Transfer System (WTS, McLane Research Laboratories, Inc. Phytoplankton Sampler) and a Digital Video Camera (DVC) [*Hill et al.*, 2011]. The LISST measures beam attenuation (Cp) and estimates particle volume concentration over a range of particle diameters. The DFC works in association with the LISST by estimating particle volume concentrations for particle diameters that are too large for the LISST to detect. Combined, the LISST and the DFC cover a range of particle diameters of 2µm -

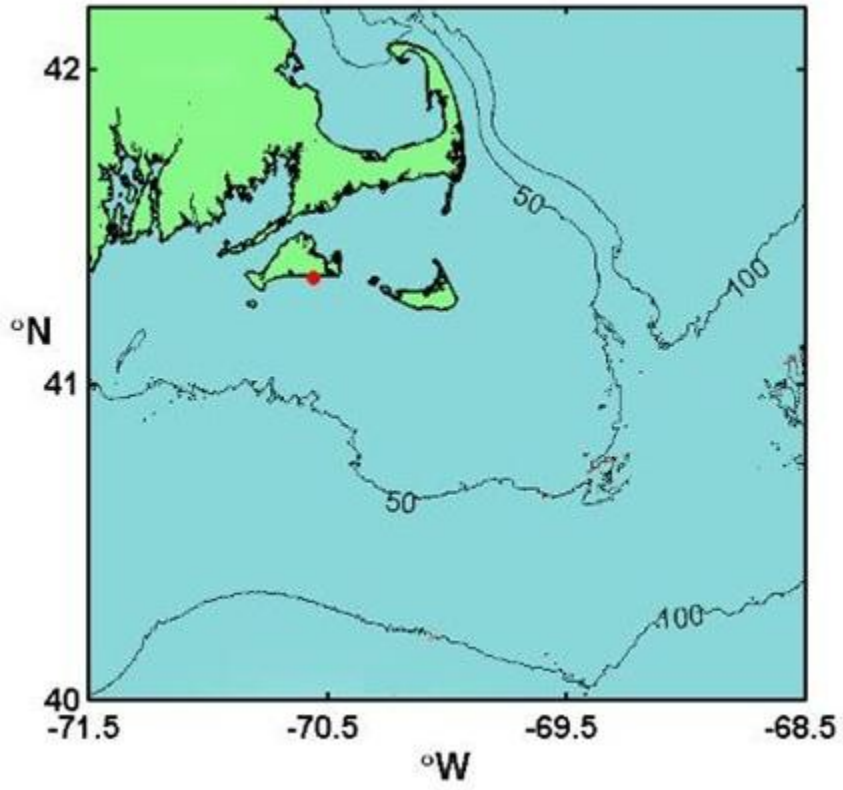

Figure 2.1: Location of the Martha's Vineyard Coastal Observatory 12-m offshore node. The red dot indicates the position of the Observatory on the south coast of the island.

4 cm. The DVC produces video clips, which are used to extract particle diameter and settling velocity data. The mounted instruments are all 1.2m above the seabed [*Hill et al.*, 2011].

The MINSSECT was deployed five times in 2007 and 2011, over a period extending from September to October. For 2007, the first deployment occurred from September 1 to September 2, the second from September 2 to 9, the third from September 10 to September 13, the fourth from September 13 to September 19, and the fifth from September 20 to September 24 [*Hill et al.*, 2011]. For 2011, the first deployment occurred from September 14 to September 21, the second from September 21 to 27, the third from September 27 to October 5, the fourth from October 5 to October 12, and the fifth from October 12 to October 19. This specific time of year was chosen for the deployments due to the range of forcing conditions that occur at this time [*Hill et al.*, 2011]. After each recovery, the windows of each instrument were cleaned of debris to reduce the risk of biofouling.

2.2.1 **LISST**

The LISST contains 32 ring detectors, which measure the intensity of light scattered by particles along a 5-cm path. The transmitted light from the source to the end of the 5-cm path is also measured. The LISST estimates volume concentration of particles at 5-min intervals with a range of diameters of 1.25 to 250 µm [*Hill et al.*, 2011; *Mikkelsen et al.*, 2005]. The distribution of light scattered onto the ring detectors is inverted with manufacturer-supplied software to determine the shape of the particle

size distribution, and the attenuation of the transmitted beam is used to estimate concentration [*Mikkelsen et al.*, 2005]. During recovery, the data are uploaded to a PC from the LISST prior to redeployment.

The WTS is used to obtain a direct estimate of suspended particulate mass (SPM) concentration. The SPM is obtained from 24 filter samples held by the WTS. At regular intervals a specified volume of a suspension is passed through an individual filter. The filters used are pre-weighed Millipore 8.0 µm SCWP (cellulose acetate). These were selected on the basis of small operational pore sizes and reduced clogging [*Hill et al.*, 2011]. Prior to deployment, the system is flushed with water to clean the tubes of any debris. The air in the WTS is then flushed out using super Q water, resulting in a temporarily sealed system. Two identical McLane water transfer systems were used and exchanged between deployments. Prior to each recovery the idle WTS was prepped and during recovery was mounted in place of the active WTS.

2.2.2 **DFC**

The digital floc camera (DFC) captures images of suspended particles with silhouette photography [*Hill et al.*, 2011; *Mikkelsen et al.*, 2004; *Mikkelsen et al.*, 2005]. The images are collected at 5-minute intervals, identical to the LISST, ensuring that they are in sync. The field of view of the DFC is a 4 x 4 x 2.5 cm slab of water that flows between two glass plates. Each pixel in an image is equal to ~15 µm and to be considered a particle, an object must be at least 9 pixels (3 x 3 pixels). The minimum resolution, therefore, is approximately 45µm [*Hill et al.*, 2011; *Mikkelsen et al.*, 2004;

Mikkelsen et al., 2005]. The captured images are stored on an internal hard drive and uploaded to a PC during a recovery [*Mikkelsen et al.*, 2004].

2.2.3 **DVC**

The DVC is mounted to a settling column for the purposes of measuring settling velocity and particle diameter. The settling column includes a mechanized lid that helps to still the fluid in the column. The lid closes 15 seconds before the capture of a video clip. The DVC is loaded with an 80-min mini Digital Video (miniDV) tape and is replaced after every deployment. The DVC records 1-minute video clips of the particles settling into the column. During recovery the miniDV tape is rewound and exchanged with a new tape. Sediment is also collected from the settling column to characterise the component-grain size distribution of settling particles. Prior to redeployment the DVC is focused using a grid on a transparency sheet.

2.3 **Data Analysis**

2.3.1 **LISST**

After the raw LISST data have been uploaded to a PC, the inversion is run to obtain volume distributions in a range of particle diameter bins [*Mikkelsen et al.*, 2005]. The software to process the data is provided by the manufacturer (Sequoia Scientific) and uses their spherical scattering property kernel matrix. The beam attenuation coefficient is calculated with the ratio of the intensity of the transmitted light to the intensity of light transmitted in sample of particle-free water [*Hill et al.*, 2011]. This

strategy accounts for attenuation due to water. Attenuation due to dissolved substances is reduced by using a wavelength of 670µm [*Hill et al.*, 2011]. As a result, the beam attenuation coefficient can be used as an estimate of the particulate beam attenuation coefficient.

2.3.2 **DFC**

After the images have been uploaded to a PC, an area of interest (AOI) is chosen for each image. An AOI is used to analyze the best area of each image, reducing the effects of debris on the window [*Hill et al.*, 2011]. Once an AOI is chosen, the original colour images are cropped to the AOI and converted to gray-scale images. A top-hat filter is applied in Matlab to the gray-scale images to smooth background pixel intensity. Particles are identified from the background in the gray-scale image by obtaining a threshold gray scale value using Otsu's method [*Hill et al.*, 2011; *Otsu*, 1979]. Equivalent spherical volumes are obtained by converting particle areas contained in each image. The equivalent spherical volumes are distributed into 35 bins based on diameter, with the lower 10 bins overlapping with the upper 10 bins of the LISST data [*Hill et al.*, 2011; *Mikkelsen et al.*, 2004]. LISST data and DFC data are combined to create a merged size distribution. Merging is achieved by simple linear interpolation between user selected neighbouring bins in the DFC and LISST spectra [*Hill et al.*, 2011].

2.3.3 **DVC**

The miniDV tapes are placed in a Digital Video Player that is connected to a Sony Vaio GRZ610 laptop, via firewire cable. The Digital Video Player works with video editing

software (Sony Imageshaker or Adobe Premier) to separate and create digital copies of each one-minute video clip. The clips are stored on an external hard drive and are saved as dv files, which are compatible with video editing software as well as QuickTime player [*Mikkelsen et al.*, 2004]. Each 1-minute clip is loaded into the video editing software (Sony Imageshaker) and is observed for settling particles for the length of the clip. After observation is complete, a suitable 4-second section of the video is chosen for each clip. Four frames, spaced 1 second apart, are captured from the section. A fifth frame is captured at the end of the video clip for the purposes of subtracting stationary debris on the settling column (Figure 2.2), such as barnacles. A Matlab script is then run on each of the 5 captured frames. A threshold is chosen to identify the gray scale that separates particles from the background [*Mikkelsen et al.*, 2004; *Fox et al.*, 2004]. The initial threshold values are determined using Otsu's method and can be adjusted by the user if the particle edges are not representative [*Otsu*, 1979]. Particles in the sequence of frames are identified, tagged, and then the frames are combined into two composite images (Figure 2.3). Particle tracks are constructed by recording the colour-coded tagged numbers. Particles in the first frame are denoted with a red number. Particles in the second, third and fourth frames are tagged with green, blue and yellow, respectively. Particle tracks with three appearances (three colour coded numbers) can be used. These numbers are recorded in a txt file for each one minute video clip. Each txt file contains 15-25 particle tracks. A second Matlab script is run to extract nominal diameter, settling distance, settling time and settling velocity from the composite images [*Hill et al.*, 2011; *Fox et al.*, 2004].

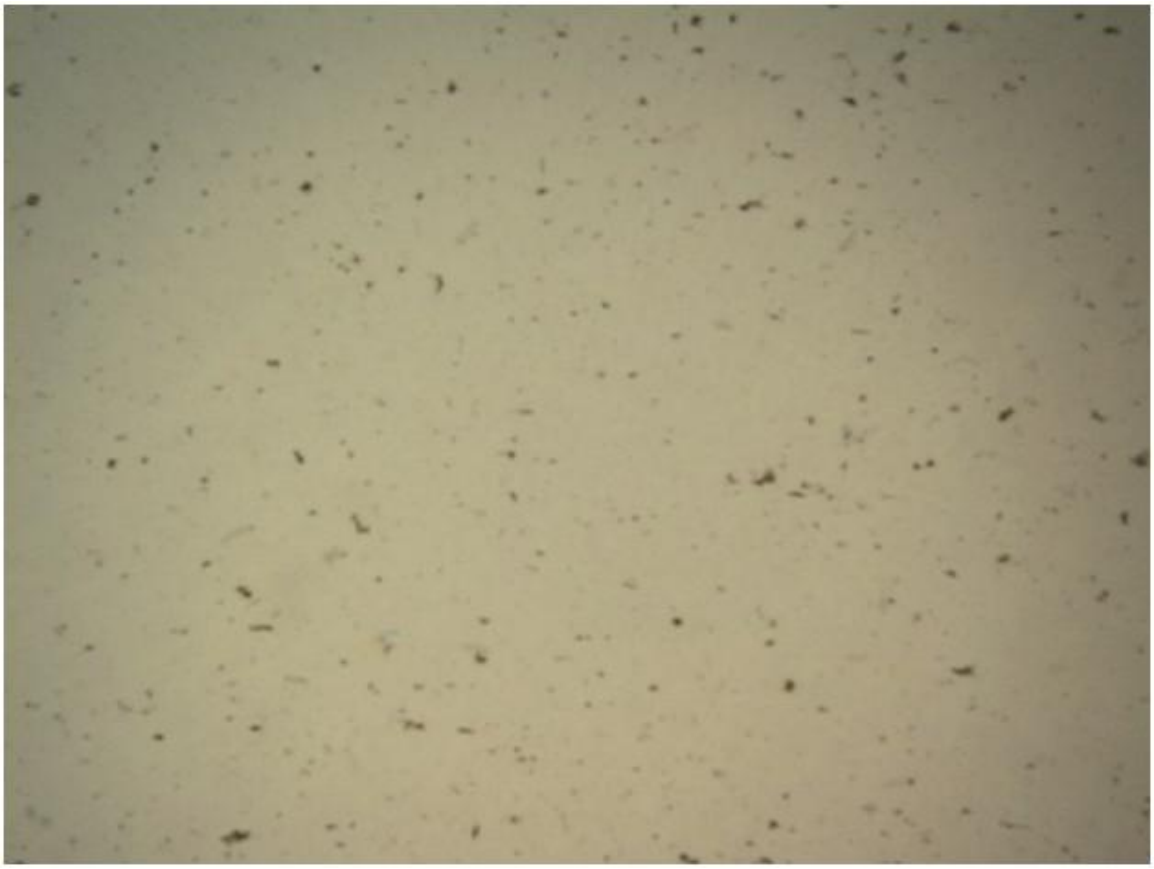

Figure 2.2: Sample image from Deployment 2, Clip 34 of the DVC. The image, is a reference frame, which is used to subtract stationary debris from the other frames sampled for analysis of particle settling velocity. The dark objects are particles. The image measures 4.1 cm across.

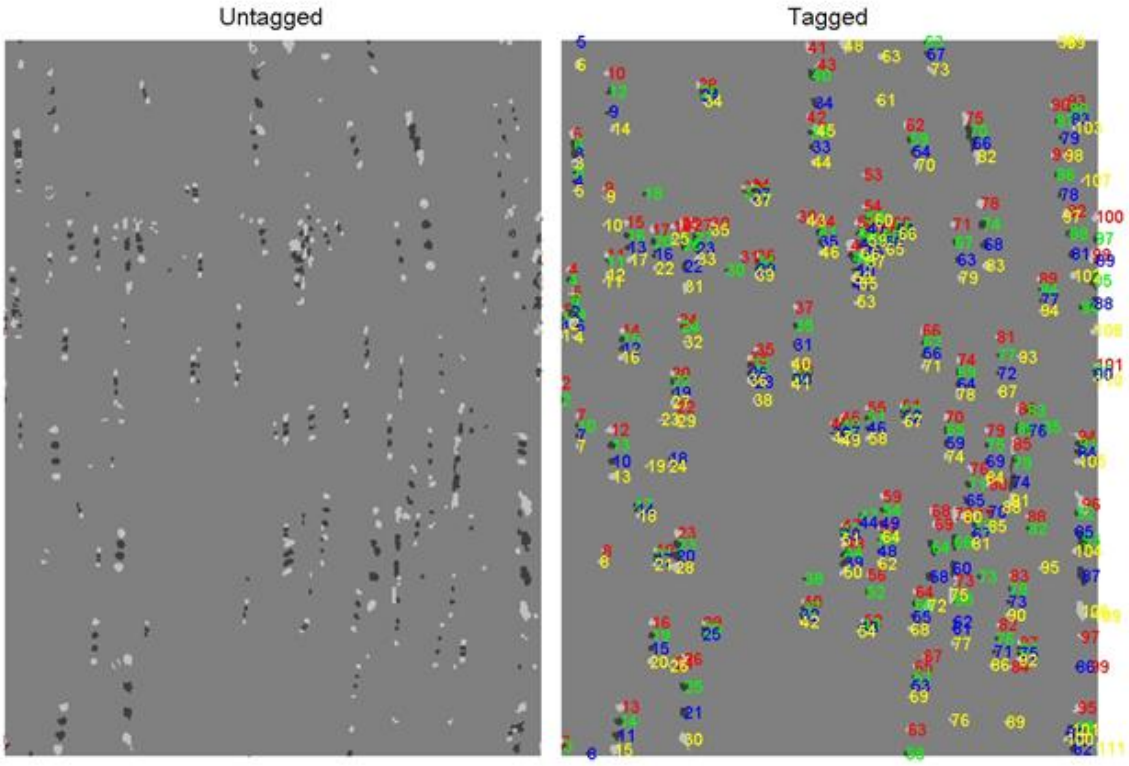

Figure 2.3: Composite images from deployment 2, clip 34: Left) Untagged composite image comprising four frames each separated by 1 second; Right) Tagged composite images where the colour of a number-tagged particle depends on the frame in which it is found. Red tags indicate frame 1. Green, blue and yellow tags indicates frames 2, 3 and 4 respectively. Particle tracks are constructed from the image with tagged particles. The numbers of the coloured tags are recorded and are used to determine settling velocity and particle size.

2.4 Density Calculations

2.4.1 DVC

Analysis of the DVC composite images provides settling velocity as well as particle size. These variables can be used to calculate particle density by using Stokes Law (equation 1). Using the settling velocity and diameter values, Stokes Law can be arranged to solve for particle density, where: ρ_S is particle density, ρ_{water} is the density of water, D is diameter, W_s is settling velocity and μ is the viscosity.

$$\rho_s = \left(\frac{\mathrm{Ws} * 18\mu}{\mathrm{g} * \mathrm{D}^2}\right) + \rho_{\mathrm{water}} \quad [1]$$

Unit conversion needs consideration in this calculation. Settling velocity (Ws) is initially measured in mm/s and is converted to m/s. Diameter is measured in micrometers and converted to meters. Viscosity, gravity and ρ_{water} are treated as constants, with corresponding units of kg $(m \cdot s)^{-1}$, m s^{-2} and kg m^{-3}, respectively.

2.4.2 LISST

The LISST measures beam attenuation (Cp), which is proportional to mass in suspension. To convert Cp to mass, a conversion factor must be used. This conversion factor is obtained by plotting measured beam attenuation (obtained using the LISST) versus in situ measurements of mass in suspension (obtained using Water Transfer System) and then calculating the slope of a linear regression of Cp on SPM, which equals Cp:SPM. The conversion of beam attenuation to mass is shown in equation (2)

$$Mass = \frac{\text{Cp}}{\text{Cp: SPM}} \quad [2]$$

Bulk density is calculated using a simple relationship of total particle mass divided by total particle volume. Beam attenuation is used to estimate solid mass per unit of volume in suspension. The mass of water contained in particles is not measured, so it is approximated as equal to the product of water density and particle volume. This approximation is justified on the grounds that the volume of flocculated marine particles is dominated by void spaces filled with water. Particle volume estimates are made by the LISST and DFC. The DFC measurements overlap upper estimates from the LISST to create merged volumes for individual class sizes. The sum of these volumes that correspond to bins 1-57 is the total particle volume concentration in suspension. To estimate particle density, the following equation is used:

$$\rho_{Merged} = \frac{Mass}{Sum\ of\ Merged\ Bin\ Volumes} + \rho_{Water} \quad [3]$$

where ρ_{Merged} is equal to bulk density and ρ_{Water} is equal to the density of water, which is calculated using salinity and temperature from the data collection site. The variable ρ_{Water} is an assumed constant throughout each deployment year. This assumption is based on the observed small range of temperature and salinities over the course of the deployments. For 2007, a constant water density of 1022.8 kg m^{-3} is used. For 2011, the variables of temperature, salinity and water density are 18.5 ^{o}C, 31.9 PSU and 1022.8 kg m^{-3} respectively.

2.4.3 **2011 Data Correction**

During deployments 1 and 2 of 2011, barnacle growth was observed on the instruments of MINSSECT. This barnacle growth affected the LISST and DFC data. The barnacle growth through deployments 1 and 2 caused the measured LISST Cp and volume concentrations to be artificially high. The barnacles also appear in the images taken by the DFC. With the advent growth, Cp increases exponentially. This is corrected by fitting an exponential function to the smoothed data and removing that exponential function from the observed Cp. The DFC images were corrected using background image subtraction, which is similar to the DVC image correction for stationary objects. This is accomplished by calculating the average pixel intensities in 6-hour bins and removing them from each image. This has the potential for artificially low volume concentrations as the portions of the images covered by barnacles cannot contain particles due to the subtraction process.

Of the 32 LISST size bins, only bins 27 and higher experienced a significant change caused by the barnacle growth. These volumes did not require correction, as the final volume concentrations used in this analysis were computed using an interpolated merge of the particle distributions. The full merged distributions are a concatenation of LISST data in bins 1-19, DFC data in bins 25-57, and linearly interpolated values in bins 20-24.

Chapter 3 - Results

3.1 DVC Results

Weather at the Martha's Vineyard Coastal Observatory during the period of data collection resulted in a variety of particle sizes and settling velocities during September and October 2011. DVC data were recovered from the first two deployments, which yielded a total of 104 video clips, with clip times in the range of 34 seconds to 1 minute 40 seconds. The number of observations per clip ranged between 15 to 25 particle tracks, which yields a total of 2242 particles observed during the deployments in 2011. During the deployments in 2007, weather forcing resulted in a variety of particle sizes and settling as well. A total of 315 video clips were collected from the series of deployments in 2007. The total number of particles observed from this series of deployments was 7606. It should be noted that current and wave forcing events were similar during both the 2007 deployment year and during the 2011 deployment year. DVC clips from both years show a wide range of suspended sediment concentration, from relatively low sediment concentrations to relatively high sediment concentrations.

Particle settling velocity is a power-law function of particle diameter [*Hill et al.*, 2011]. The exponent and 95% confidence intervals in the relationships are 0.68 ± 0.03 and 0.78 ± 0.07 for the 2007 and 2011 data respectively (Figure 3.1). These exponents are not significantly different. Mean and median settling velocities for 2011 are 1.1385 mm s^{-1} and 0.8235 mm s^{-1}, while the 2007 data contain mean and median settling velocities of 1.3855 mm s^{-1} and 1.0553 mm s^{-1}. The exponent is less than the value of 2,

appropriate for particles of constant density due to the fact that particles in suspension are aggregates, with densities that decrease with increasing size (Figure 3.1) [*Hill et al.*, 1998; *Agrawal and Pottsmith*, 2000]. Particle diameters span similar ranges for both years, with the 2011 data ranging from 226.1 μm to 1776.6 μm and the 2007 data ranging from 220.9 μm to 1973.3 μm.

3.2 **LISST Results**

The relationship between beam attenuation and SPM for the 2007 data has been outlined by *Hill et al.* [2011]. Beam attenuation (Cp) plotted against SPM results in a linear relationship, with the slope equal to the Cp:SPM ratio. This ratio is used to solve for mass in suspension by dividing beam attenuation by the Cp:SPM ratio (equation 2). For the 2007 data, this value, plus or minus two standard deviations is 0.22 ± 0.0015 m^2g^{-1} [*Hill et al.*, 2011]. Beam attenuation and measured particulate mass have been plotted again for the 2007 data. The resultant slope is 0.23 ± 0.02 m^2g^{-1}, which is similar to the findings of *Hill et al.* [2011], with a variance of 0.01 m^2g^{-1} between the newly plotted data and the data plotted by *Hill et al.* [2011] (Figure 3.2). For the purposes of this research, the value of 0.22 described by *Hill et al.* [2011] is used as the conversion value and is assumed constant for the 2007 dataset. A linear relationship between beam attenuation and measured particulate mass also applies to the 2011 dataset (Figure 3.3). The slope of the 2011 regression is 0.38 ± 0.08 m^2g^{-1}. The difference between the coefficients in 2007 and 2011 is significant, so separate conversions of Cp to SPM are applied. The slopes for each dataset fall within the 0.2-0.6 $m^2\ g^{-1}$ range observed by *Boss et al.* [2009] in a study across multiple environments.

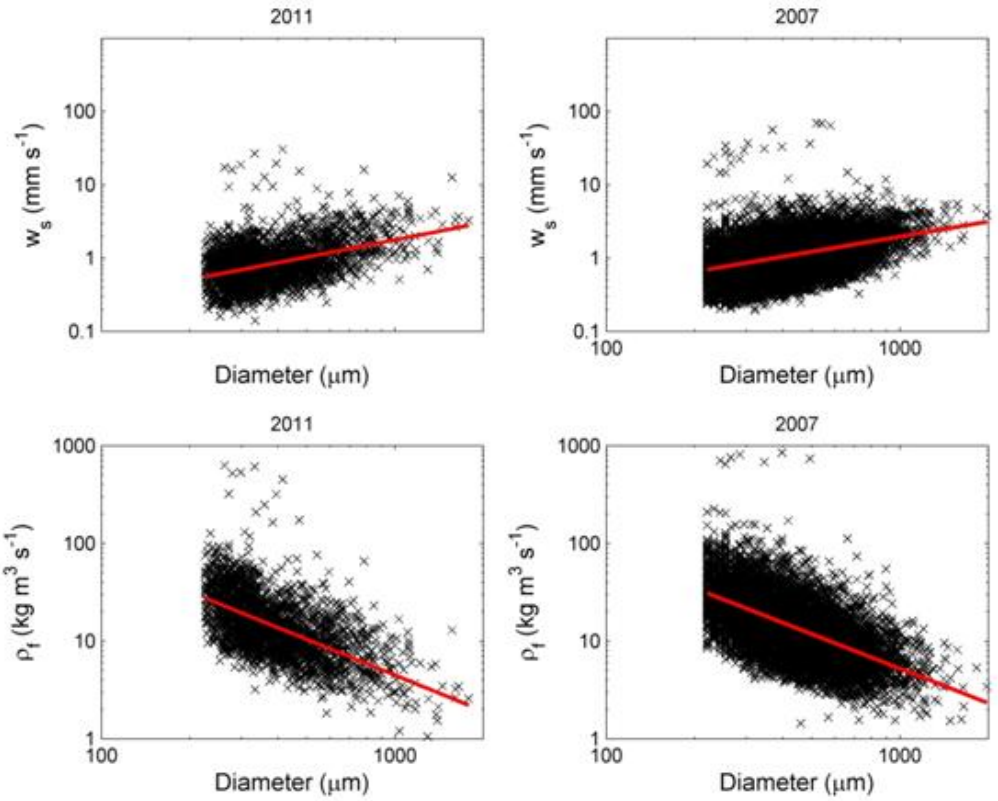

Figure 3.1: Top Panels) Log-log plots of settling velocity vs. Diameter for 2011 (left) and 2007 (right). Bottom Panels) Log-log plots of effective particle density vs. diameter for 2011 (left) and 2007 (right). The red lines are best-fit linear regressions. Slopes with confidence intervals are reported in the text.

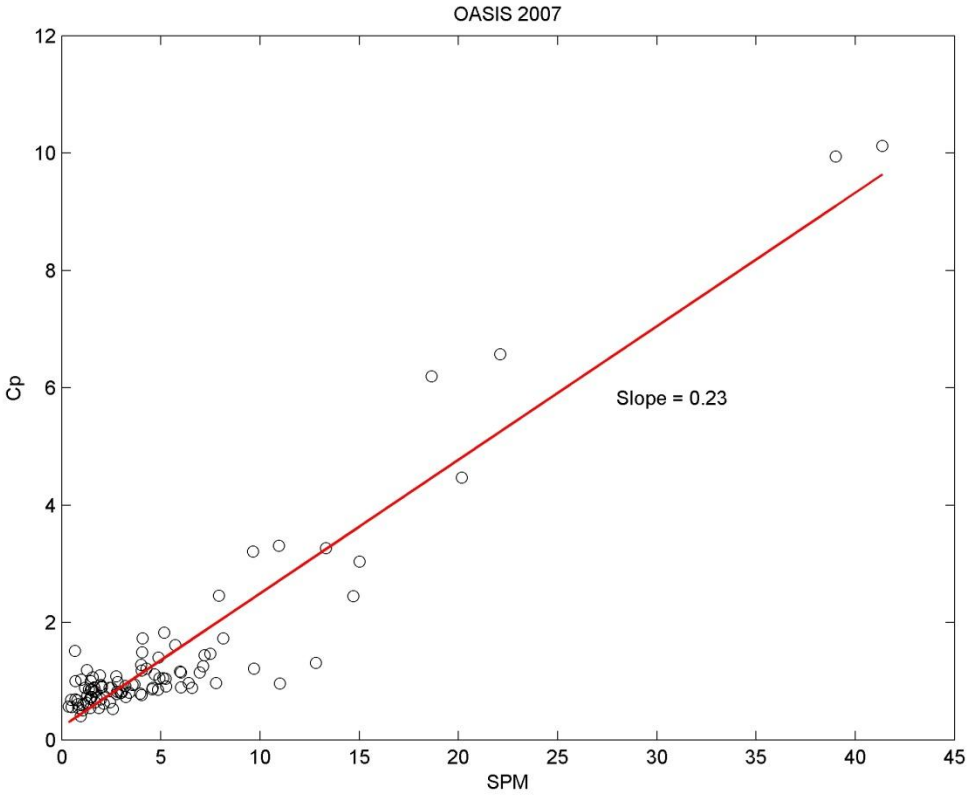

Figure 3.2: Beam attenuation (Cp,m^{-1}) versus in situ measurements of mass (g m^{-3}) for 2007. The slope of the line, which is called the Cp:SPM ratio, is equal to 0.23 ± 0.02 m^2g^{-1}.

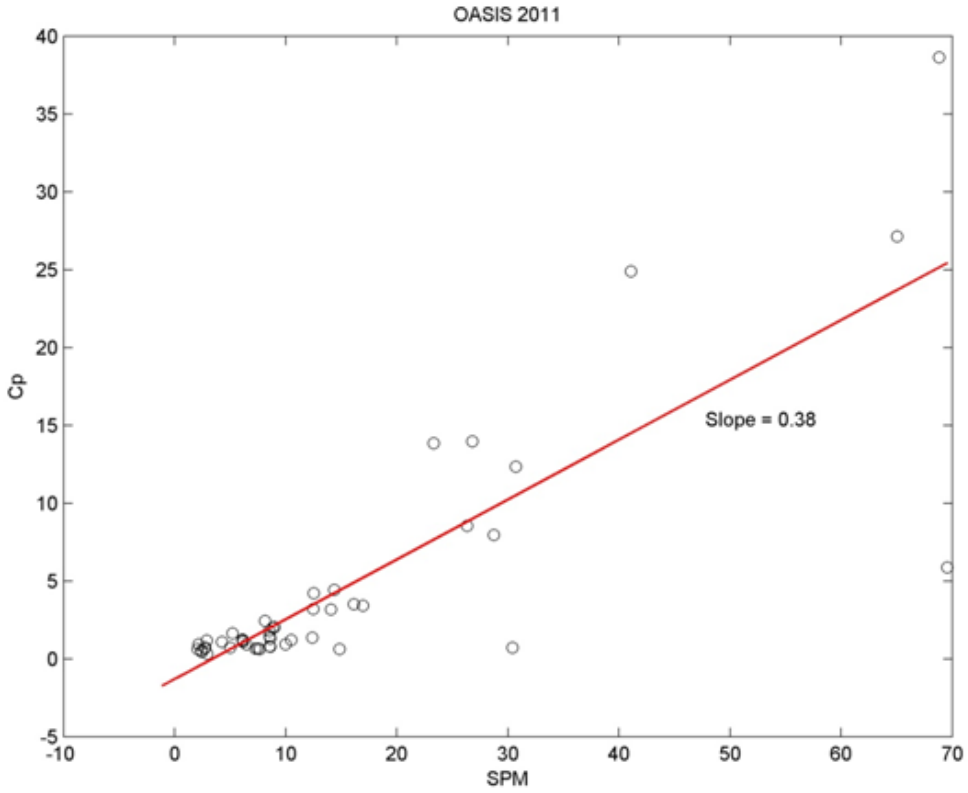

Figure 3.3: Beam attenuation (Cp, m^{-1}) versus in situ measurements of mass (g m^{-3}) for 2011. The slope of the line, which is called the Cp:SPM ratio, is equal to 0.38 ± 0.08 $m^2 g^{-1}$.

3.4 **Particle Density versus Merged Bulk Density**

Particle bulk densities estimated with the two methods provide results that vary between 2007 and 2011. For the 2007 dataset, the particle densities estimated using each method do not agree. Particle densities estimated with the DVC vary between 1027.1 kg m^{-3} and 1164.4 kg m^{-3}, while bulk densities estimated with the LD method are much larger, ranging between 1124.3 kg m^{-3} and 2480.3 kg m^{-3}. The data fall well below the expected 1:1 relationship and exhibit no linear relationship (Figure 3.4). Conversely, the 2011 dataset shows a linear relationship that is close to the hypothesized 1:1 relationship. The particle densities in 2011 from the DVC method range from 1027.0 kg m^{-3} to 1064.0 kg m^{-3} and the majority of bulk densities from the LD method range from 1124.3 kg m^{-3} to 1400.0 kg m^{-3}, with only five points larger than this range (Figure 3.5). The differing density comparisons between years poses a new question as to why the years are so different.

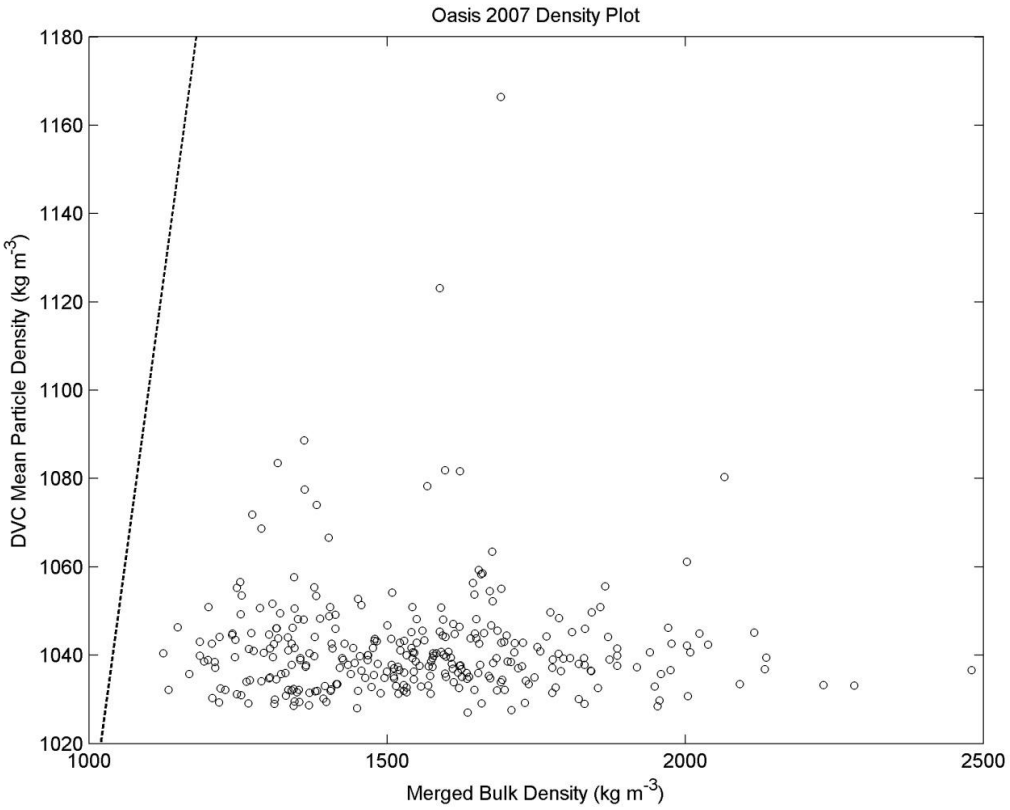

Figure 3.4: Mean particle density (DVC method) vs. merged bulk density (LD method) for 2007 dataset. Data fall well below the dashed 1:1 line, indicating that the LD method produces larger density estimates than the DVC method. No relationship between the DVC densities and the LD densities is apparent.

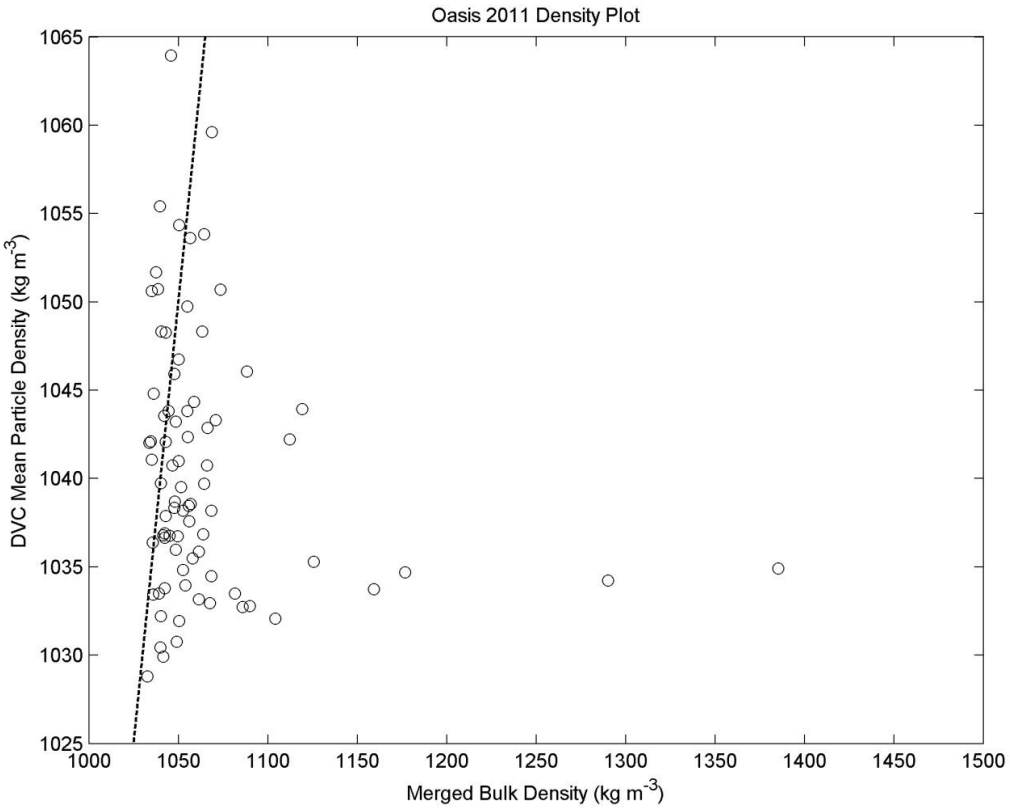

Figure 3.5: Mean particle density (DVC method) vs. merged bulk density (LD method) for 2011 dataset. Data fall near the dashed 1:1 line.

Chapter 4 - Discussion and Conclusion

4.1 Discussion

The two density comparisons from 2007 and 2011 have results that disagree. The densities obtained using each method in the 2011 dataset generally follow a 1:1 relationship, indicating that the LD method is an accurate alternative to the DVC method. The density comparison from 2007, however, shows significant scatter and the data fall much below the 1:1 relationship. There is not a significant linear relationship between the two estimates of bulk density. The reasons why the comparisons vary require investigation.

The diameter and settling velocity data collected from the DVC during the 2007 and 2011 deployments are similar (Figure 4.1). This consistency of DVC data between deployment years suggests that the source of disagreement in density comparisons is associated with the LD method. Wave and current action was similar during the deployments in 2007 and 2011, therefore external forcing is likely not the cause of variance in the datasets. The higher densities in the 2007 series of deployments may be due to higher beam attenuation or to lower volume than measured in 2011. Comparison of the measured beam attenuations in each year shows that they lie within the same range, thus suggesting that different measurements of particle volume between years cause the differing estimates of density (Figure 4.2). This hypothesized cause for higher densities in 2007 is supported by the observation that measured particle volumes were systematically lower in 2007 than in 2011 (Figure 4.2).

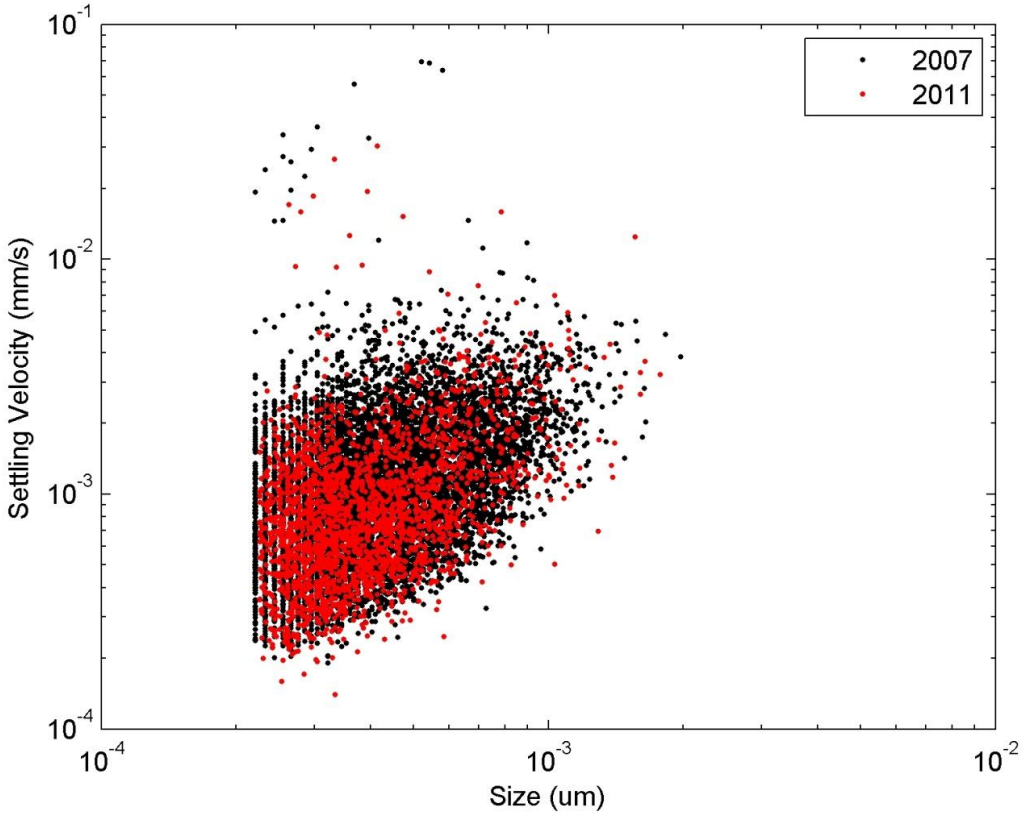

Figure 4.1: Settling velocity and diameter obtained from the DVC. The 2011 data overlap the 2007 data, indicating that the DVC functioned similarly in the two years.

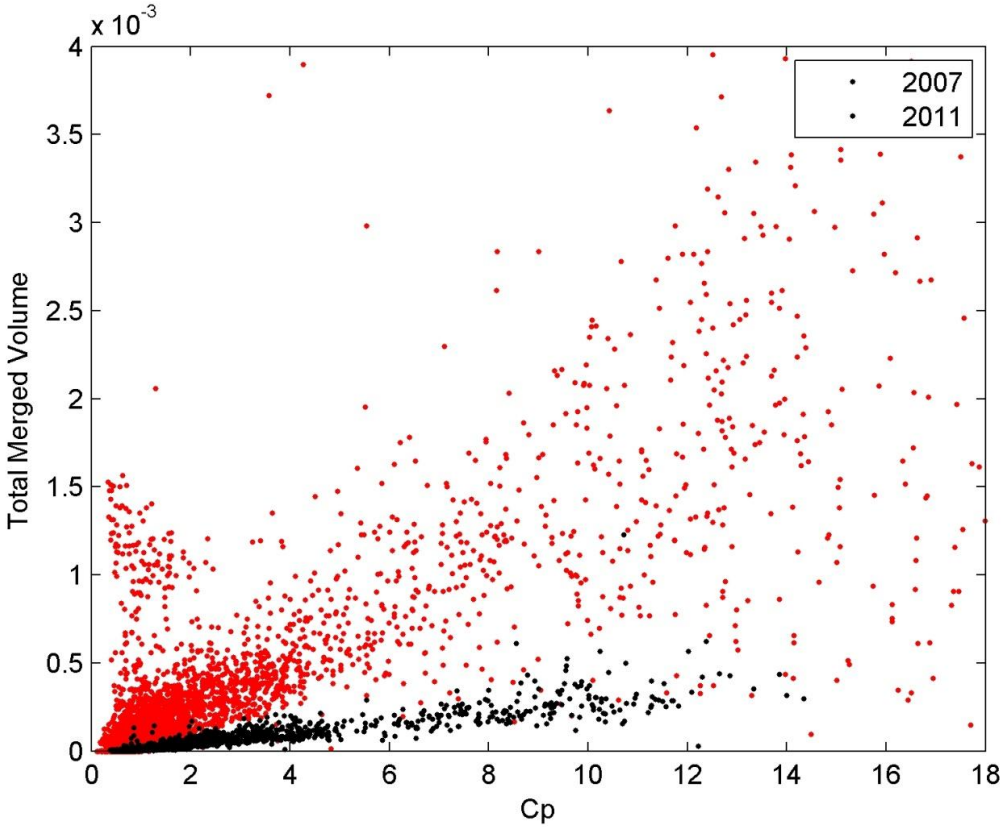

Figure 4.2: Total Merged Volume plotted against Cp for the 2007 and 2011 datasets. Beam attenuation (Cp, m^{-1}) measurements fall in the same range for both years. The total merged volume (m^3 m^{-3}) is significantly lower in the 2007 dataset, which explains higher density estimates, as volume appears in the denominator in the formula for bulk density.

Observations of the DFC images and corresponding size distributions for lower concentration periods and higher concentration periods for 2007 (Figures 4.3 and 4.4) and 2011 (Figures 4.5 and 4.6) indicate that the DFC is the source for the lower volumes in 2007. The LISST beam attenuation and volume concentration measurements from 2007 and 2011 are in a similar range, suggesting that the volumes from the LISST are accurate. To create the merged particle volume distributions, DFC volumes are combined with LISST volumes (Figures 4.3- 4.6). The DFC volume data cover diameters above approximately 100 μm in the merged distributions where most of the particle volume in the distribution resides. In 2007, DFC volumes are almost an order of magnitude smaller for similar forcing conditions than they are in 2011 (Figures 4.3-4.6).

There are four possibilities for why the DFC volumes are lower in 2007. The first possibility is technical issues with the digital floc camera. The camera may not have been properly focused or the lens may not have been clean during the series of deployments in 2007. However, care is taken during recovery and redeployment to clean the lenses and the focus is fixed.

A second possibility is poor water clarity during the series of 2007 deployments. If water clarity is poor, clarity of the DFC images may suffer. The clarity of the water could have been reduced by higher concentrations of light-absorbing coloured dissolved organic matter (CDOM) in the water during the 2007 deployments. Research on light absorption due to increased CDOM has shown that an increase in light absorption is related to an increase in CDOM [*Woodruff et al.*, 1999]. Therefore, more light absorption due to increased CDOM may reduce the quality of images taken by the DFC.

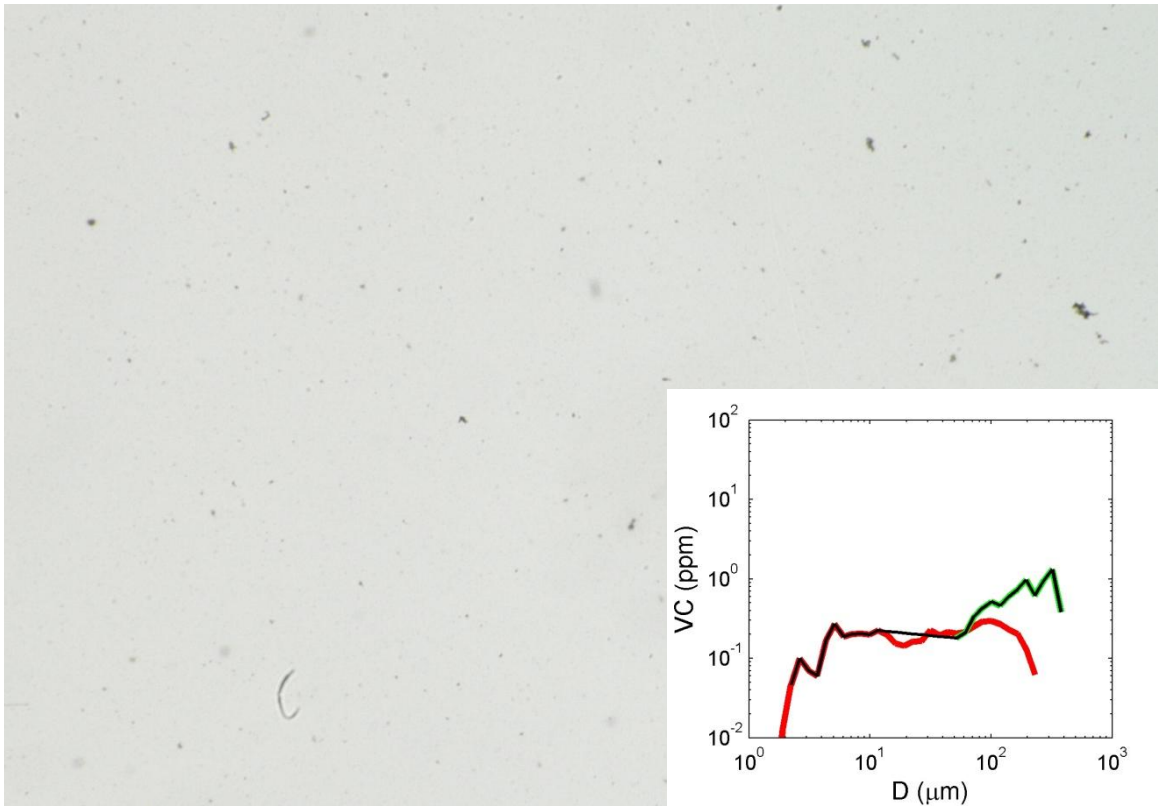

Figure 4.3: Low concentration DFC image and corresponding size distribution from the 2007 dataset, yearday 264. The width of the image is 40 mm. The inset shows the merged particle size distribution, with diameter on the x-axis and volume concentration in parts per million on the y-axis. Bulk density calculated for this time is at the upper end of the LD bulk densities.

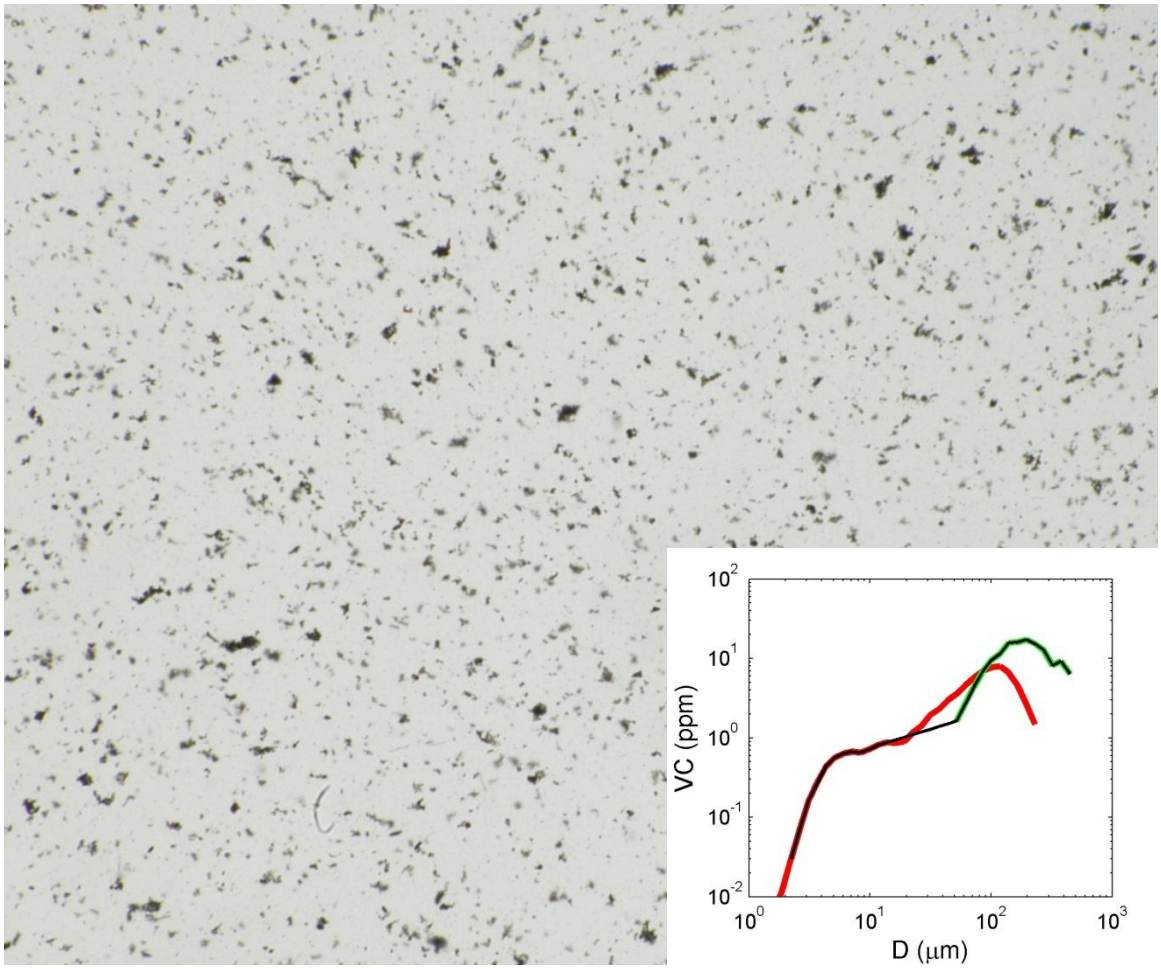

Figure 4.4: High concentration DFC image and corresponding size distribution from the 2007 dataset, yearday 256. The width of the image is 40 mm. Bulk density with the LD method for this image falls at the lower end of the range estimated bulk densities.

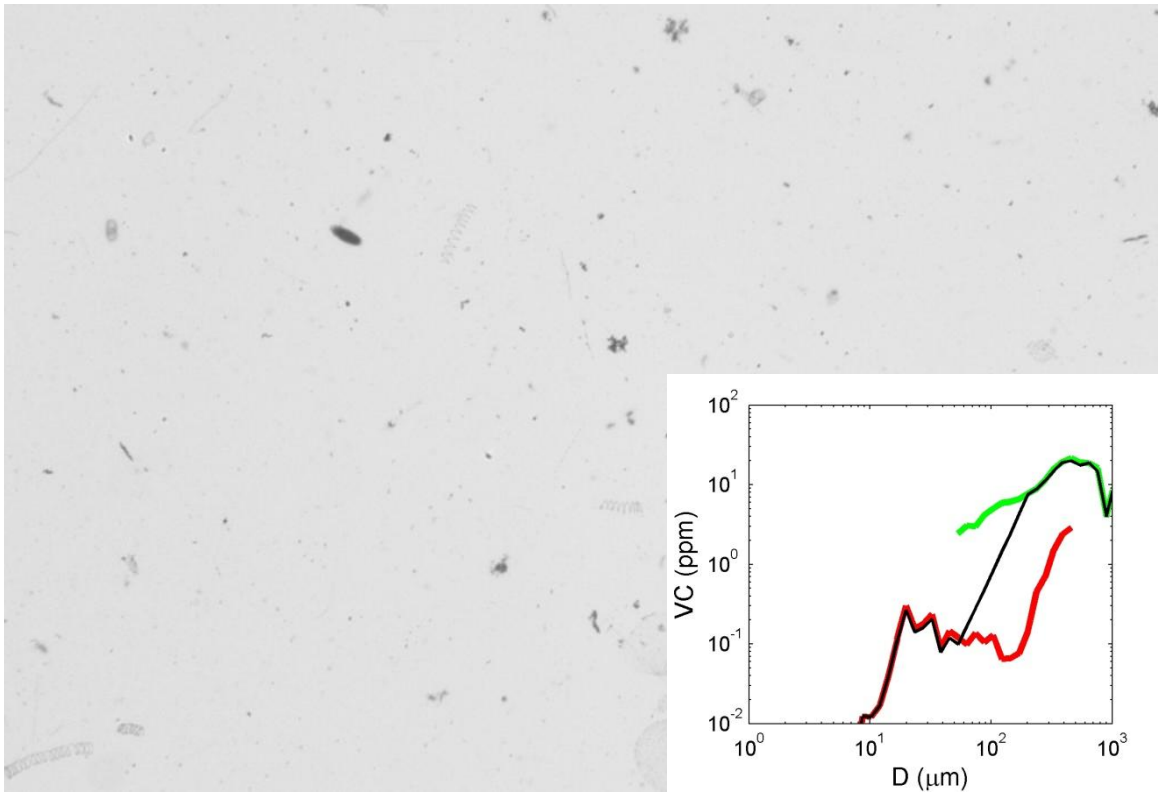

Figure 4.5: Low concentration DFC image and corresponding size distribution from the 2011 dataset, yearday 265. The width of the image is 40 mm. Relatively large concentrations of large, light-coloured, presumably organic flocs can be observed in addition to smaller, darker, inorganic flocs. Densities estimated by both methods are similarly low for this image.

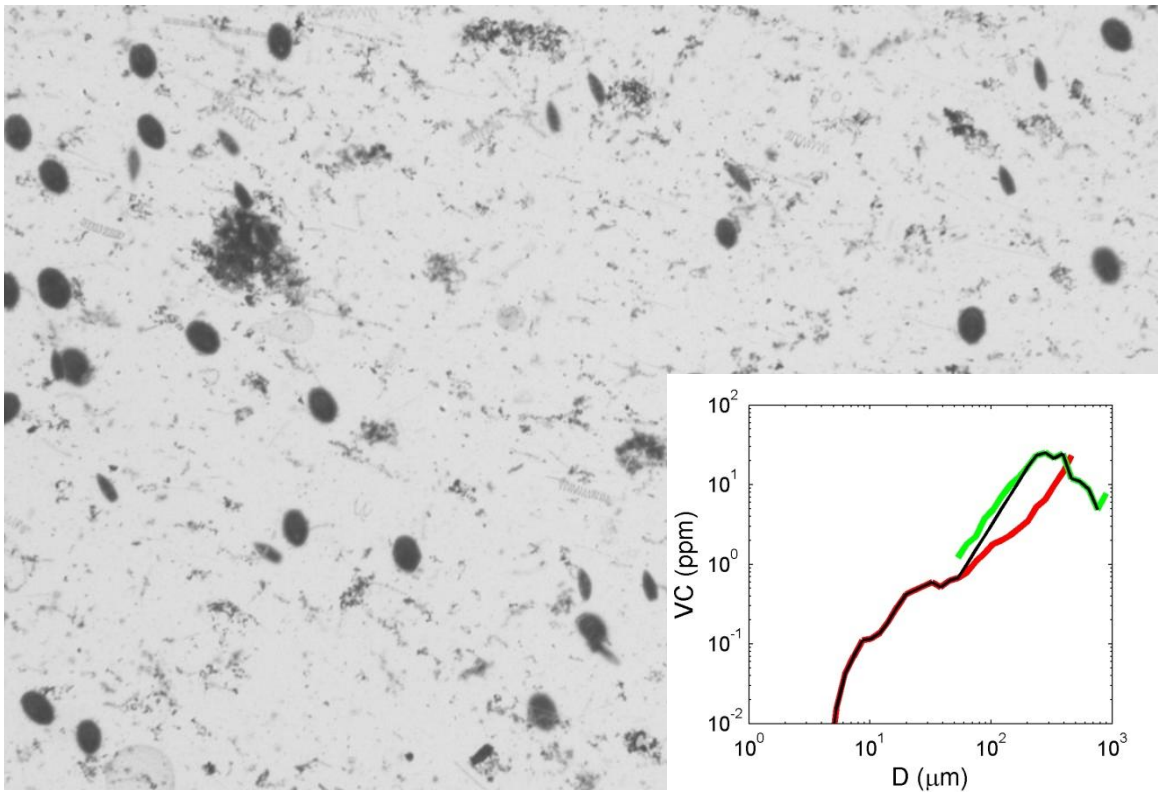

Figure 4.6: High concentration DFC image and corresponding size distribution from 2011 dataset, yearday 262. The width of the image is 40 mm. Barnacles appear as dark ovoids in the image. The effects of barnacle growth on the LISST beam attenuation and DFC volume concentration are removed. See text for details. Densities estimated by both methods are similarly low for this image.

CDOM data may be available from colleagues who made measurements at the MVCO 12-m during the series of deployments conducted during 2007 and 2011. Therefore, comparison of coloured dissolved organic matter between the two years could be carried out in the future.

A third possibility for lower DFC volumes in 2007 involves the optical properties of the particles. Perhaps the particles present in 2007 have refractive indices closer to that of water, making them more difficult for the DFC to image clearly. Research by *Babin et al.,* [2003] has shown that in coastal regions relatively low scatter amongst suspended particulate mass is common. The Cp:SPM ratio for particles with a small refractive index would be lower than for particles with a larger refractive index, as observed between 2007 and 2011. The approximate factor-of-two difference in Cp:SPM ratios between years indicates that different particle optical properties may account for some of the differences in DFC volumes.

A final possibility for different DFC volumes between the years is that the differences are real. In 2007, large flocs may have been much rarer. The DVC can only measure large flocs, so the density estimated with the DVC in 2007 may be unrepresentative of the majority of particles in that year, which could have been smaller and denser. In 2011 large flocs may have dominated the size distribution, so DVC estimates of density are more representative. This hypothesis could be examined by deriving a density model for all particle sizes based on the DVC data [*Khelifa and Hill*, 2006], then multiplying bin-specific densities by volume in each bin of the merged distributions [*Hill et al.*, 2011]. If the DFC volumes in 2007 are accurate, then the

resulting density estimates should be closer to the bulk densities estimated with the beam attenuation and merged volume distributions.

4.2 **Time Series**

Despite uncertainty regarding the accuracy of density measurements, examination of time series of density and other variables demonstrate potential future applications of the method. Time series of shear velocity, beam attenuation and densities (LD method and DVC method) contain information about each parameter during different stages of the deployments (Figure 4.7). Measurements of shear velocity were made by colleagues at the MVCO 12-m during the series of deployments conducted in 2007 and 2011. When shear velocity increases, an increase in beam attenuation is also observed. This is logical because as shear velocity increases, the sea bed undergoes increased stress, which suspends more particulate matter, thus increasing beam attenuation. This relationship is also observed in density time series. For 2007, observed densities, especially from the LD method, decrease as stress increases. This observation suggests that during resuspension events larger flocs, which are less dense, are in suspension. For 2011, observed LD densities increase slightly when stress increases. This observation suggests that during 2011 there is resuspension of denser material during high stress events, likely small flocs that have undergone compaction in the seabed.

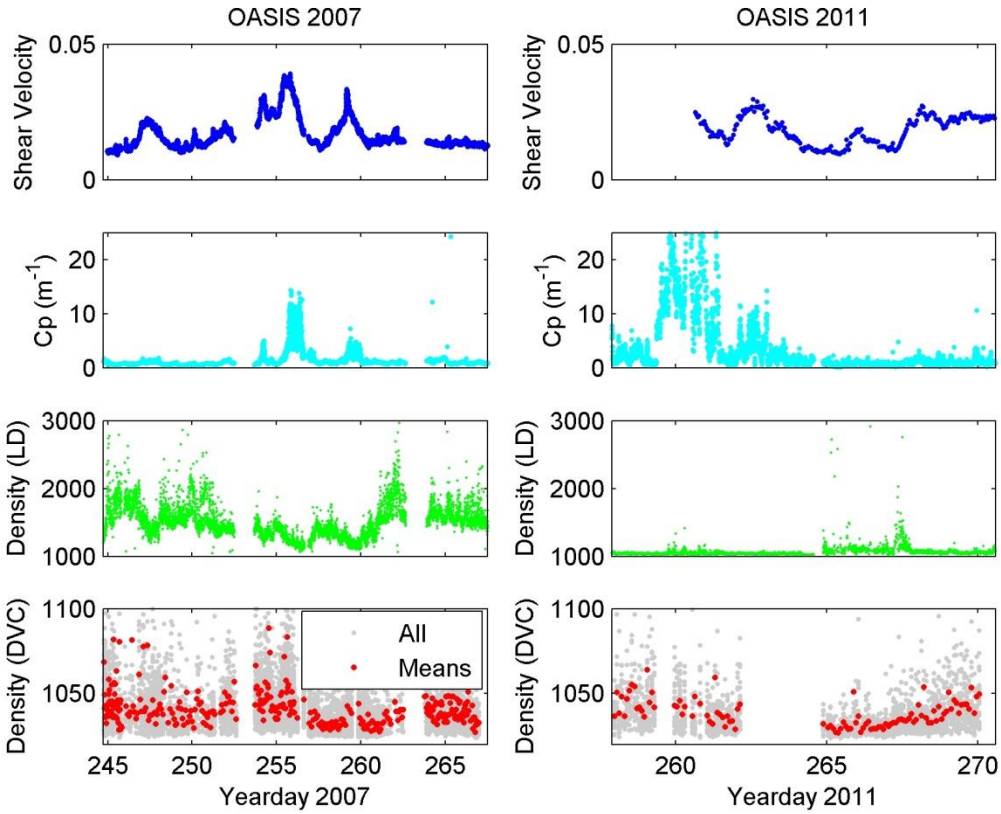

Figure 4.7: Time series plots for the 2007 (left panels) and 2011 (right panels) datasets. The x-axis in the plots remains constant and represents sample times for 2007 and 2011. Plots contain comparisons of shear velocity (cm s^{-1}), beam attenuation (Cp, m-1), bulk density estimated from the LD method (kg m^{-3}) and particle bulk density estimated from the DVC method (kg m^{-3}). The final panels represent estimated Density from the DVC method, where grey points are all of the collected data points and the red points are the mean densities during each data collection interval.

4.3 **Future Work**

The fundamental issues raised by the comparison of bulk density estimates are accuracy of the DFC and representativeness of the DVC. To examine whether water clarity affects the accuracy of the camera, correlations between light attenuation due to dissolved substances (if available) and DFC volume should be examined in the data from 2007 and 2011. Alternatively, the DFC could be used in the laboratory to image particles with different refractive indexes in water of differing concentrations of dissolved substances. Such a controlled experiment would reveal whether there is systematic bias in estimated DFC volumes caused by changing particulate and dissolved optical properties. The representativeness of the DVC densities could be examined as previously described with existing data. Finally, more data from other sites would help to clarify the accuracy of particle bulk densities based on Cp and merged volume distributions. Increasing the library of datasets would be beneficial in determining if an error that caused lower volumes is exclusive to 2007 or if varying DFC volumes among deployments are typical, which would indicate that obtaining density relationships may require improved imaging technology.

4.4 **Conclusion**

It is unclear if the new method of calculating bulk density using the LISST and DFC is an accurate alternative to the DVC method for non-invasive, in situ estimation of particle bulk density. The data collected in 2011 suggests that there is a possibility that the LD method may offer similar density results as the DVC method. The dataset from 2007 contradicts this finding. Various explanations may account for the lower DFC volume concentrations in 2007 that result in higher density estimates. Additional research is required to determine if the LD method for calculating bulk density is comparable to the DVC method for obtaining bulk density.

Referenced Literature

Agrawal, Y.C. and H.C. Pottsmith (2000), Instruments for particle size and settling velocity observations in sediment transport, *Marine Geology, 168,* 89-114.

Babin, M, A. Morel, V. Fournier-Sicre, F.Fell and D. Stramski (2003), Light scattering properties of marine particles in coastal and open ocean waters as related to the particle mass concentration, *Limnology and Oceanography, 48,* 843-859.

Baker, E.T. and J.W. Lavelle (1984), The effect of particle size on the light attenuation coefficient of natural suspensions, *Journal of Geophysical Research, 89,* 8197-8204.

Boss, E., et al. (2009), Comparison of inherent optical properties as a surrogate for particulate matter concentration in coastal waters, *Limnology and Oceanography Methods, 7,* 803–810.

Fox, J.M., P.S. Hill, T.G. Milligan, A.A. Ogston and A. Boldrin (2004), Floc fraction in the waters of the Po River Delta, *Continental Shelf Research, 24,* 1699-1715.

Hill, P.S, E. Boss, J.P. Newgard, B.A. Law and T.G. Milligan (2011), Observations of the sensitivity of beam attenuation to particle size in a coastal bottom boundary layer*, Journal of Geophysical Research, 116,* C02023, 1-14.

Hill, P.S., J.P. Syvitski, E.A. Cowan, R.D. Powell (1998), In situ observations of floc settling velocities in Glacier Bay, Alaska, *Marine Geology, 145(1-2),* 85-94.

Khelifa, Ali and Paul S. Hill (2006), Models for effective density and settling velocity of flocs, *Journal of Hydraulic Research, 44(3)*, 390-401.

Mikkelsen, O. A., T.G. Milligan, P.S. Hill, D. Moffatt (2004), INNSECT - An instrumented platform for investigating floc properties close to the seabed, *Limnology and Oceanography-Methods, 2*, 226-236

Mikkelsen, O. A., T.G. Milligan, P.S. Hill, R.J. Chant (2005), In situ particle size distributions and volume concentrations from a LISST-100 laser particle sizer and a digital floc camera, *Continental Shelf Research, 25(16)*, 1959-1978

Ogston, A.S., R.W. Sternberg (1999), Sediment-transport events on the northern California continental shelf, *Marine Geology, 154,* 69-82

Otsu, N. (1979), A threshold selection method from gray-level histograms, *IEEE Trans. Syst. Man Cybern., 9(1),* 62–66.

Woodruff, D.L., R.P. Stumpf, J.A. Scope and H.W. Paerl (1999), Remote estimation of water clarity in optically complex estuarine waters, *Remote Sensing of Environment, 68*, 41-52.

Appendices

Appendices are contained in Microsoft Excel format on the attached CD-ROM.